Contributions of benthic microalgal biofilms to sediment organic carbon stocks across a salt marsh gradient

Underwood, G. J. C. ORCID: https://orcid.org/0000-0001-5605-0697, Slee, N. J. D. ORCID: https://orcid.org/0009-0006-6354-5624, Underwood, J. C. J. ORCID: https://orcid.org/0009-0006-6761-2134, Underwood, C. I. D. ORCID: https://orcid.org/0000-0002-1691-6377 and Pinckney, J. L. ORCID: https://orcid.org/0000-0002-6056-6511 (2026)
Contributions of benthic microalgal biofilms to sediment organic carbon stocks across a salt marsh gradient. Limnology and Oceanography, 71 (1). e70303. ISSN 1939-5590 doi: 10.1002/lno.70303 Available at https://centaur.reading.ac.uk/127749/

LIMNOLOGY and OCEANOGRAPHY

ASLO

Limnol. Oceanogr. 71, 2026, e70303

doi: 10.1002/lno.70303

RESEARCH ARTICLE

Contributions of benthic microalgal biofilms to sediment organic carbon stocks across a salt marsh gradient

Graham J. C. Underwood [1*], **Nicola J. D. Slee** [1], **Jessica C. J. Underwood** [2], **Christopher I. D. Underwood** [3], **James L. Pinckney** [4]

[1]School of Life Sciences, University of Essex, Colchester, Essex, UK; [2]School of Archaeology, Geography and Environmental Science, University of Reading, Reading, UK; [3]Independent Scientist, Bristol, UK; [4]Estuarine Ecology Laboratory, Department of Biological Sciences, and School of the Earth, Ocean, and Environment, University of South Carolina, Columbia, South Carolina, USA

Abstract

Benthic microalgal (BMA) communities contribute significantly to food webs, nutrient cycling, and carbon flows in intertidal habitats. However, the contribution of BMA to saltmarsh carbon stocks ("blue carbon") is unclear. BMA and sediment total organic carbon (TOC) stocks were measured in an east coast American Atlantic saltmarsh, revealing key relationships between biofilm biomass, carbohydrate, and carbon content. BMA biomass (chlorophyll *a*) was highest in *Sporobolus* stands and mudflat habitats, with diatoms the dominant algal group, and cyanobacteria more important in upper saltmarsh sites. Habitat-specific differences in biofilm properties (biomass, carbohydrates, photopigments, near-infrared spectra) corresponded to differences in overall contributions to sediment TOC. Carbohydrates contributed between 8% and 23% of sediment TOC, with the highest levels in *Sporobolus* and mudflat habitats. BMA biomass and colloidal carbohydrate were significantly correlated, except on lower shore sandflats. The greatest relative contribution of colloidal carbohydrate to %TOC was in upper marsh and tidal channel habitats (1%). Mudflats had the highest %TOC (up to 5% dry weight), but TOC stocks (2000 g C m^{-2} to a depth of 10 cm) were highest in *Sporobolus* habitats. A modeling approach, based on LIDAR and sediment measures, determined a BMA carbon contribution of 1.3–8% of sediment TOC, with the lowest values in *Sporobolus* and mudflat habitats. Upscaling from m^2, incorporating habitat heterogeneity, gave median values of 14–16 t TOC ha^{-1} for the North Inlet Estuary saltmarshes, of which BMA contributed 0.06–0.08 t C ha^{-1}. This approach could permit BMA contributions to blue carbon to be estimated across other saltmarshes.

Salt marshes are recognized as important "blue carbon" habitats acting as long-term sinks for sequestered atmospheric CO_2 at rates equivalent to seagrass beds, terrestrial forests, or the open ocean (Adams 2020; Mason et al. 2023). Reported salt marsh sediment organic carbon stocks and accumulation rates vary widely, depending on location, type of marsh, and assumptions regarding the distribution of carbon in the top 1 m of sediment (Chen and Lee 2022; Mason et al. 2023; Mazarrasa et al. 2023). Salt marshes also serve as receiver habitats for allochthonous organic carbon imported from land and sea (Walden et al. 2024). Salt marshes exist in a dynamic equilibrium with adjacent tidal flats (Ladd et al. 2019; Redzuan and Underwood 2020), and unvegetated tidal flats also contain significant stocks of organic carbon with high potential annual accumulation rates (Chen and Lee 2022; Mazarrasa et al. 2023; Mason et al. 2023). Areas of unvegetated sediment within salt marshes are also a potentially significant reservoir of organic carbon (Chen and Lee 2022).

Benthic microalgal biofilms (BMA), assemblages of autotrophic and heterotrophic protists, bacteria, archaea, and fungi, are abundant in intertidal systems and contribute significantly to ecosystem primary production, nutrient cycling, food webs, and act as sediment stabilizers and ecosystem engineers (Pinckney 2018; Cibic et al. 2019; Hope et al. 2020; Underwood et al. 2022). Though rates of BMA primary production are well researched, the net contribution of BMA to sediment

*Correspondence: gjcu@essex.ac.uk

Associate editor: Oscar Serrano

organic carbon stocks is less well understood. BMA make a significant contribution to the overall carbon economy of salt marsh environments (Hardison et al. 2013; Oakes and Eyre 2014; Frankenbach et al. 2020). BMA biofilms are present on sediment among vascular halophytes (e.g., *Sporobolus* sp., synonym *Spartina*) and on unvegetated sediments. BMA annual net primary production typically ranges between 29 and 314 g C m^{-2} y^{-1} (Pinckney 2018; Kwon et al. 2020), with the abundance and species composition of salt marsh BMA exhibiting zonation patterns in relation to tidal height, exposure, sediment composition, and nutrient loading (Nedwell et al. 2016; Plante et al. 2020; Kwon et al. 2020; Underwood et al. 2022). BMA biomass is also correlated with sediment particle size, with particle size a proxy for sediment carbon content and porewater nutrient supply (Cibic et al. 2019; Redzuan and Underwood 2020; Martins et al. 2022).

In the North Inlet Estuary, South Carolina, BMA provided 22–38% of the total ecosystem net primary production (NPP), with contributions from phytoplankton and the halophyte *Sporobolus* at 15–26% and 30–59%, respectively (Pinckney and Zingmark 1993b). Similar high BMA NPP contributions have been measured in other estuaries (Cahoon 1999; Frankenbach et al. 2020; Haro et al. 2020), despite low standing stocks of BMA biomass. Photosynthetic activity by BMA produces extracellular polymeric substances (EPS), polysaccharide-rich material that can be dissolved, colloidal, or relatively insoluble (Bellinger et al. 2005, 2009; Underwood 2024). There are well-described relationships between BMA biomass (Chlorophyll *a*) and colloidal carbohydrate concentrations (Underwood and Smith 1998; Thornton et al. 2010) and more refractory carbohydrates (Bellinger et al. 2005; Hardison et al. 2013; Kim et al. 2021) in intertidal biofilms. However, these relationships vary in different intertidal habitats (sandy to muddy; temperate to tropical) (Cook et al. 2007; Oakes et al. 2010, 2012) and with biofilm type (Underwood and Smith 1998; Bellinger et al. 2005; Thornton et al. 2010; Kim et al. 2021; Underwood et al. 2022).

Carbohydrates are an important component of the carbon stock in unvegetated sediments, and microalgal activity is a significant factor in determining the concentrations of total and colloidal carbohydrates. The turnover times of different carbon stocks vary due to differential bacterial utilization of low molecular weight, colloidal, and bound (insoluble) forms (McKew et al. 2013; Bohórquez et al. 2017; Underwood et al. 2022). The potential for sequestration of BMA organic carbon also depends on sediment characteristics, with finer sediments enabling greater carbon preservation due to greater surface areas providing more binding sites and slower remineralization rates under anaerobic conditions (McKew et al. 2013; Chen and Lee 2022; Walden et al. 2024). Infrared spectroscopy has the potential to characterize BMA carbon, as Near and Mid-infrared spectroscopy (NIR and MIR, respectively) can identify unique spectral features linked to chemical composition and stocks of organic material in soils, salt marsh, mangrove, and seagrass sediment (Yang 2020; Song et al. 2022; Walden et al. 2024).

Saltmarshes are currently the focus of extensive research in determining their role as "blue carbon" habitats. In this study, we investigated the contribution of BMA to sediment total organic carbon (TOC) stocks in the surface sediments of the North Inlet Estuary (NIE), South Carolina, United States. The NIE is typical of the extensive salt marshes along the southeastern seaboard of North America, dominated by *Sporobolus alterniflorus* (syn. *Spartina alterniflora*) and containing a mosaic of vegetated and unvegetated habitats across the tidal height gradient. The BMA biomass–carbon relationship is less studied in North American salt marshes (Thornton and Visser 2009; Thornton et al. 2010) compared to European and East Asian intertidal habitats (*op. cit.*). This study provides new data to expand our understanding of the contributions of BMA biofilms to coastal "blue carbon" and develops a modeling and upscaling approach that would be applicable to other similar habitats. The primary objectives were:

1. To measure the relationships between BMA biomass (sediment Chl. *a*) and biofilm parameters (total, colloidal carbohydrate) across a range of habitats and sediment types (vegetated and unvegetated, sands, silts, muds) within the NIE.
2. Use these relationships to determine the contribution of BMA carbon to sediment organic matter and total organic carbon (TOC) content.
3. Develop an approach to model sediment TOC concentrations and BMA contributions to TOC across saltmarsh habitat gradients to obtain landscape-scale carbon stock estimates.

Methods

The NIE, South Carolina, United States (Fig. 1) is a large (33 km^2) euhaline (25–40 salinity) bar-built system, like many other estuaries in the southeastern United States (Dame et al. 2000) and is part of the U.S. National Estuarine Research Reserve (NERR) network. The NIE has semidiurnal tides (average tidal range 1.4 m) with approximately 70% of the estuarine water volume exchanged with each tide (Allen et al. 2014). The freshwater input is mainly from a 3800 ha protected forest watershed, with some coastal housing developments to the north of the reserve. The NIE is composed of an extensive tidal creek system with fringing mudflats bordered by the saltmarsh cordgrass *S. alterniflorus* (Supporting Information Fig. S1). Sediments are mineralogenic, primarily fine to very fine sands (median $\varphi = 2.7$–3.8), and the percent silt ($\varphi = 4$–8) and clay ($\varphi > 8$) ranges from 1% to 40% (by dry weight) (Pinckney and Zingmark 1993a; Wigand et al. 2015). The intertidal area and BMA habitat of NIE is ca. 3000 ha.

Benthic microalgal biofilms were sampled from 11 sites, representing 6 different habitat types (Supporting Information

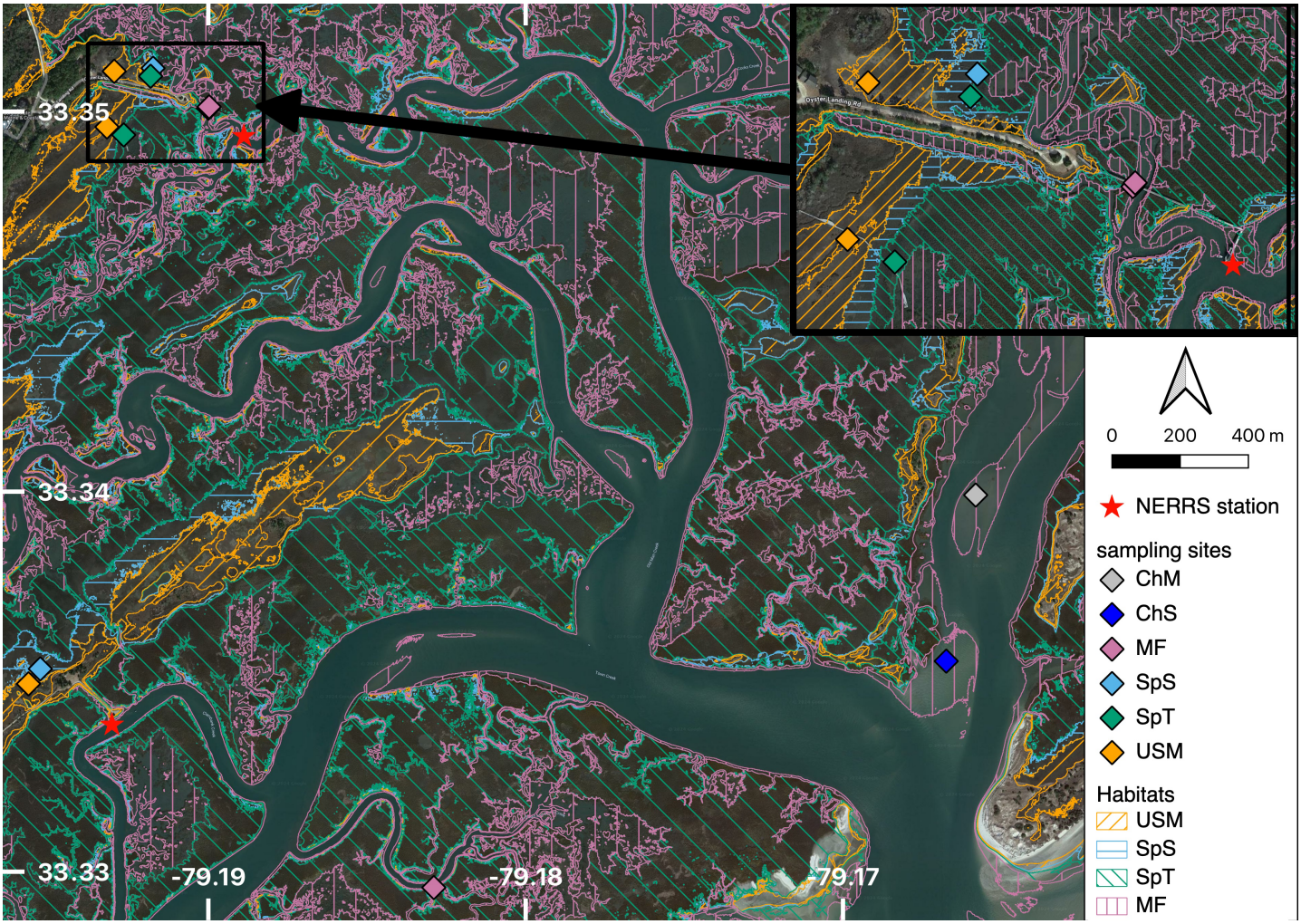

Fig. 1. North Inlet Estuary (NIE), South Carolina, United States, showing the spatial distribution of four major habitat types (derived from NOAA height data), and sites and habitat type at each sample location (*see* Supporting Information Table S1). USM = upper salt marsh, SpT = tall *Sporobolus* and SpS = short *Sporobolus* marsh, MF = unvegetated mudflat, ChS = channel sandflat, and ChM = channel mudflat habitats. The location of NERRS water quality monitoring stations is indicated. The inset box shows the locations of sites in the Oyster landing locality. Image from GoogleEarth July 2024.

Fig. S1; Supporting Information Table S1), from the upper intertidal salt marsh (Upper Salt Marsh, USM), sparsely vegetated with *Sporobolus* and *Juncus* and colonized by sand fiddler crabs *Leptuca pugilator* (Pinckney 2023); the short and tall vegetation zones of *S. alterniflorus* (SpS and SpT, respectively); intertidal mudflats in creek systems (mudflat, MF); and lower shore main channel sandflats (ChS) and mudflats (ChM) (Fig. 1; Supporting Information Fig. S1; Supporting Information Table S1). Sampling took place during a wet summer period (July 2018) and a drier winter season (February 2023) (Supporting Information Table S2).

At each site, pairs of sediment cores (taken adjacent to each other) were sampled using plastic mini cores (internal diameter 2 cm) and the surface 5 mm of sediment retained. Ten replicate pairs of cores were taken randomly over an area of approximately 400 m^2 at each site, spaced at least 2 m apart. One sample from each pair was kept cool in the field, frozen within 2 h of sampling, and freeze-dried and homogenized for subsequent subsampling of biofilm properties. The second sample of the pair was dried on the day of sampling to determine sediment water content (90 °C for 24 h) and sediment organic matter determined by % loss-on-ignition (550 °C for 1 h, %LOI). In February 2023, a set of additional 10 cm depth, 2 cm i.d. paired sediment cores were taken ($n = 3$ pairs in each habitat). Three depth sections were taken: surface (0–5 mm), mid (45–50 mm), and bottom (95–100 mm), and processed as above.

Subsamples of freeze-dried biofilm samples were measured spectrophotometrically for Chl. *a* and phaeopigment content (using 100% methanol extraction, Stal et al. 1984), and for sediment total and colloidal carbohydrate concentrations using a modified phenol sulfuric acid assay to maximize

hydrolysis of polysaccharides (Aslam et al. 2012) (Supporting Information Methods).

Biofilm samples taken in 2018 were analyzed by HPLC for photosynthetic pigment concentration (Supporting Information Methods). ChemTax (version 1.95) was used to estimate the relative concentrations of major algal groups (e.g., diatoms, cyanobacteria, green algae) based on measured photopigment concentrations (Higgins et al. 2011).

Freeze-dried sediment surface and depth-core samples from 2023 were measured for total carbon (TC), total inorganic carbon (TIC), and total organic carbon (TOC) on a Skalar Primacsmcs model 2MC10900 coupled to a FormacsHT model 2CA16910-02 carbon analyzer (Skalar Analytical B.V., Beda, NL). TOC was calculated by subtraction of TIC from TC, and values were expressed as % w/w content. Near-infrared (NIR) spectroscopy measurements were also carried out on freeze-dried 2023 samples of surface sediment (Supporting Information Methods).

The tidal height data for each sample point (derived from its latitude and longitude) were extracted using NOAA's Topographic Lidar data. NOAA's lidar data has a spatial resolution of 1 m^2 and a 4.3 cm standard deviation for vertical accuracy. Meteorological measurements and water nutrient concentrations were obtained from NOAA's National Estuarine Research Reserve System's (NERRS) National Monitoring Program (https://coast.noaa.gov/digitalcoast/data/nerr.html) for three sites in the NIE (Supporting Information Table S2) for 8 d before and including the time of fieldwork.

Data analysis

Samples were coded by site, habitat type and year. Habitat types were determined by visual observations, knowledge of the site (Allen et al. 2014) and particle size analyses (Pinckney and Zingmark 1993a). Comparison between sites and habitat types was conducted in R (R Core Team 2024) using non-parametric Kruskal–Wallis χ^2 and Wilcoxon rank sum exact tests. Storm damage prevented access for repeat sampling of 2018 sites in 2023 (only OLC was sampled twice), so inter-year comparisons were made at the habitat level. Relationships among sediment variables were determined (for the combined 2018 and 2023 data set) using single and multiple linear regression, with site or habitat as factors. Relationships between sediment %LOI, colloidal and total carbohydrate contents, and direct measures of %TOC were determined using linear regression analysis (2023 data). We derived %TOC values from %LOI values by applying conversion models from a North Carolina salt marsh (Craft et al. 1991), a Portuguese estuary embayment (Martins et al. 2022), and a global tidal marsh data set (Maxwell et al. 2023). These derived %TOC values were compared using linear regression with the measured %TOC in the 2023 data set to select the best model for determining %TOC from the %LOI data for the combined data set.

To model and map sediment carbon stocks at m^2 and hectare scales, the relationships between sediment %TOC, sediment bulk density and tidal elevation were determined and used in combination with LIDAR data, the distribution of habitat types by tidal range, and our data. The contribution of BMA to sediment organic carbon stocks (g BMA TOC m^{-2}) was modeled from relationships between colloidal and total carbohydrate, protein, and lipid content of microalgae, field measurements for each habitat type, and the sediment carbon model (*see* Supporting Information Methods for approach and equations used).

Results

Differences in BMA biomass and sediment carbohydrate concentrations between habitats

Sediment Chl. *a* content varied from 1.2 to 75.3 μg g^{-1} sediment, with significant differences between sites and between habitat types (Kruskal–Wallis $\chi^2 = 106.81$, df = 10, $p < 0.001$; $\chi^2 = 90.42$, df = 5, $p < 0.001$, respectively) (Fig. 2a). Upper salt marsh sites (Supporting Information Table S1) had lower Chl. *a* content than the *Sporobolus* marsh and mudflat habitats, with the highest Chl. *a* content in the fine sediment of creek mudflat sites (Wilcoxon, $p < 0.001$ for all pairwise comparisons). There were some site-specific differences (e.g., Chl. *a* content at site OLC2018 was lower than at site OLC2023, $p < 0.01$) (Fig. 2a). The channel sand and channel mudflat sites had lower Chl. *a* content (Wilcoxon, $p < 0.01$ for pairwise comparisons) than sites within the main salt marsh. Areal measures of Chl. *a* concentration (derived using site sediment bulk density values; Supporting Information Fig. S2a) were also significantly different between habitats, with the highest concentrations (50–110 mg Chl. *a* m^{-2}) in the *Sporobolus* habitats (SpT, SpS), and similar Chl. *a* concentrations between USM and MF creek sites ($\chi^2 = 54.40$, df = 5, $p < 0.001$; Supporting Information Fig. S3a).

Sediment colloidal carbohydrate content varied from 33 to 736 μg gluc. equiv. g^{-1} sediment, with differences between sites and between habitat types (Kruskal–Wallis $\chi^2 = 98.2$, df = 10, $p < 0.001$; $\chi^2 = 80.6$, df = 5, $p < 0.001$, respectively) (Fig. 2c), which mirrored the patterns of differences seen for sediment Chl. *a* content (Wilcoxon, $p < 0.001$). The *Sporobolus* and mudflat habitats had higher colloidal content, with no significant differences between habitats, and only a few differences in colloidal content between sites (Fig. 2c). Areal concentrations of colloidal carbohydrate were highest in short *Sporobolus* (SpS) habitats (Kruskal–Wallis $\chi^2 = 39.7$, df = 5, $p < 0.001$; Supporting Information Fig. S3b).

Sediment total carbohydrate content ranged from 375 to 37,880 μg gluc. equiv. g^{-1} sediment and also showed significant differences between sites and habitat types (Kruskal–Wallis $\chi^2 = 109.3$, df = 10, $p < 0.001$; $\chi^2 = 95.7$, df = 5, $p < 0.001$, respectively; Fig. 2e). Areal concentrations of total carbohydrate (Supporting Information Fig. S3c) were highest

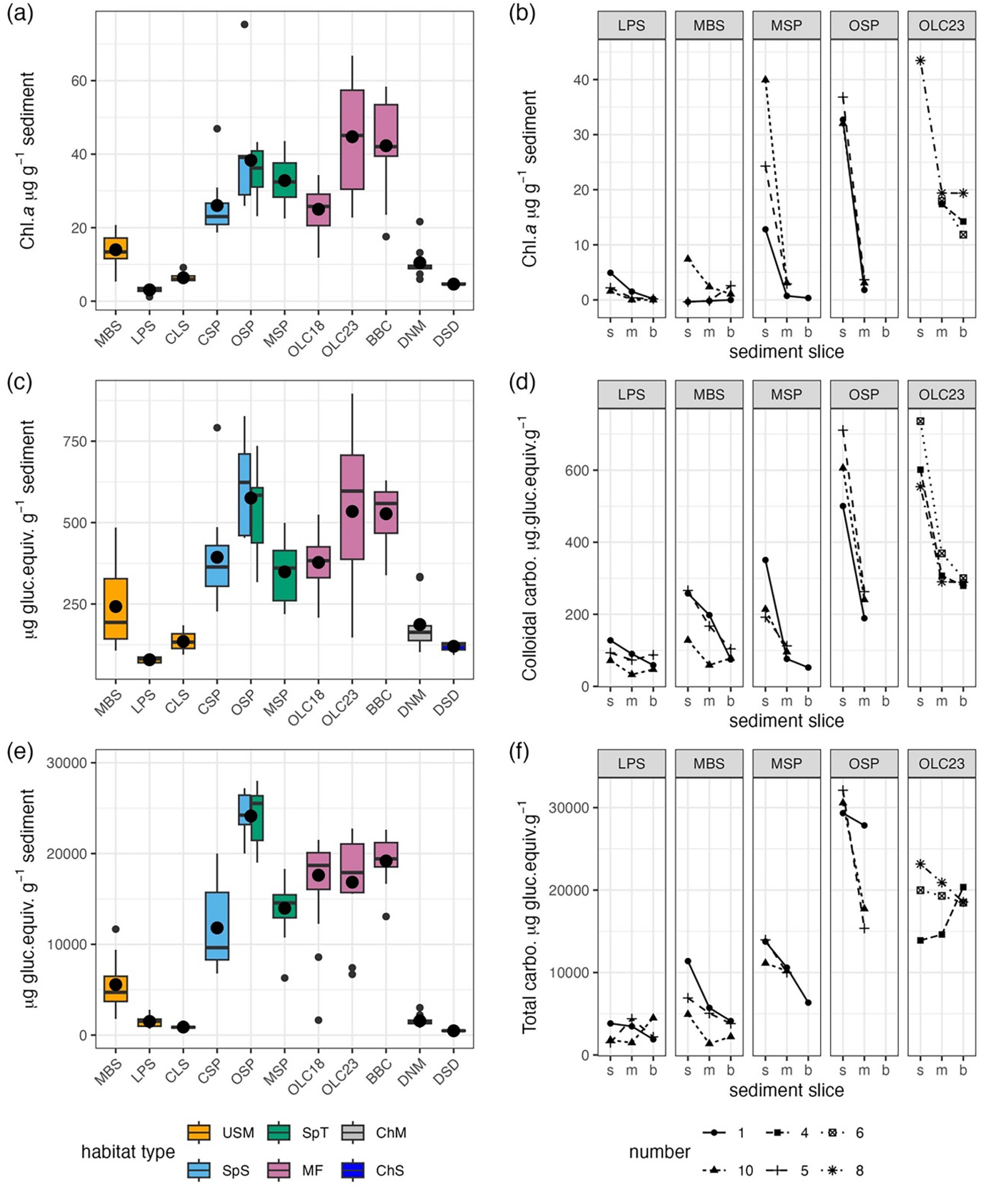

Fig. 2. Legend on next page.

in *Sporobolus* habitats (SpS, SpT), followed by mudflat (MF), upper salt marsh, and channel sand and channel mud flats, respectively (Kruskal–Wallis $\chi^2 = 87.7$, df = 5, $p < 0.001$). At site OLS, Chl. *a* and colloidal carbohydrate content were lower in 2018 compared to 2023. Overall, there were no consistent patterns in habitat comparisons between years, though temperature, salinity, and nutrient concentrations did differ (Supporting Information Table S2).

Sediment Chl. *a*, colloidal carbohydrate, and total carbohydrate content were maximal at the surface and decreased down to a depth of 10 cm (Fig. 2b,d,f, respectively). The greatest decreases occurred at depths of 0–5 mm and 45–50 mm in *Sporobolus* and mudflat habitats. Chl. *a* and colloidal carbohydrate content exhibited the greatest decreases with depth (Fig. 2b,d). In contrast, total carbohydrate content decreases were less pronounced (Fig. 2f). Thick mats of *Sporobolus* roots at site OSP prevented cores from being taken to 10 cm depth.

Colloidal carbohydrate contributed between 6.7% and 25.7% of the total sediment carbohydrate pool, with significantly higher contributions in upper salt marsh sediment and channel sand and mud sites, compared to *Sporobolus* and intertidal mudflats (Supporting Information Fig. S4A; Kruskal–Wallis $\chi^2 = 98.6$, df = 5, $p < 0.001$). Highest ratios of Chl. *a*: phaeopigment were found in USM and ChS habitats (Supporting Information Fig. S4b). There was a positive relationship between the % contribution of colloidal carbohydrate to total carbohydrate content and the Chl. *a*: phaeopigment ratio ($p < 0.001$; Supporting Information Fig. S4b) of biofilms, indicating a close link between production of colloidal carbohydrates and biofilm photosynthesis.

ChemTax analysis (Supporting Information Fig. S4c–g) found that diatoms contributed between 77% and 93% of the total chlorophyll content, with chlorophytes and euglenophytes (chl *b*-containing microalgae) contributing around 17% in the short *Sporobolus* and mudflat assemblages. Cyanobacteria contributed more to total Chl. *a* in upper salt marsh sediments and mudflats than within *Sporobolus* stands or channel sediments (Supporting Information Table S3). De-epoxidation ratios (diatoxanthin content/(diatoxanthin content + diadinoxanthin content)) were highest in mudflat (sites OLC18, BBC) and *Sporobolus* sediments (site CSP) (Kruskal–Wallis $\chi^2 = 18.4$, df = 5, *p*-value = 0.01; Supporting Information Fig. S4g).

Relationships between benthic microalgal biomass and sediment carbohydrate and organic matter concentrations

There was a significant positive relationship between sediment Chl. *a* and colloidal carbohydrate content (Fig. 3a; all sites, $\mathrm{Log}_{10}[n + 1]$ data, $F_{1,173} = 448.6$, $p < 0.001$, $r^2 = 0.72$). The slopes (β coefficient) of these relationships were significant for each habitat type ($p < 0.01$ or less, except ChM). They increased down shore, with the highest β coefficients in mudflat and channel sandflat habitats (Supporting Information Table S3). The slopes (β coefficients) were significantly lower in all six habitats compared to Underwood and Smith's (1998) model (*t*-test, $p < 0.001$ for all). There was also a significant relationship between sediment total carbohydrate content and Chl *a* content (Supporting Information Fig. S5a) combining all sites and habitat types ($F_{1,173} = 195.6$, $p < 0.001$, $r^2 = 0.53$). This relationship was significant for short and tall *Sporobolus* sediment ($p < 0.001$) and intertidal mudflats ($p < 0.01$), but not for USM, ChS and ChM habitats.

Sediment organic matter (%LOI) ranged from 0.4% to 19.3% (Supporting Information Fig. S2b) with significant differences between sites (Kruskal–Wallis $\chi^2 = 115.39$, df = 10, $p < 0.001$), with highest %LOI in mudflats, then *Sporobolus* habitats, and the lowest in channel sands (Kruskal–Wallis $\chi^2 = 105.68$, df = 5, $p < 0.001$). Sediment water content was highest in MF and SpT sites (average 65%), lowest in USM sites (20%) (Supporting Information Fig. S2c), and was significantly correlated with %LOI ($r = 0.97$, $p < 0.001$).

Derived values of sediment %TOC from %LOI using the models of Craft et al. (1991) and Maxwell et al. (2023) had significant linear relationships with direct measurements of % TOC made in 2023. Both models overestimated %TOC by factors of 1.7 and 1.6, respectively (Supporting Information Fig. S5b,c). The model of Martins et al. (2022) estimated sediment %TOC with a slope of 1 to the measured %TOC 2023 data (Fig. 3b). Using the Martins et al. (2022) model, sediment %TOC for the combined NIE dataset (years 2018 and 2023) was calculated from %LOI (Supporting Information Fig. S2b), resulting in %TOC values from 0.14% to 5.1% (Supporting Information Fig. S2d), with significant differences between sites and habitats corresponding to those for the %LOI data (Supporting Information Fig. S2b). There was a significant binomial relationship between tidal height and derived %TOC for the upper salt marsh, short and tall *Sporobolus*, and mudflat samples across the NIE ($r^2 = 0.73$; Fig. 3c; Supporting Information Methods). Data for ChS and ChM sediments did not fit this model and were excluded from its further use.

Sediment total carbohydrate (converted into carbon equivalents) contributed 8–23% of the TOC stock, with significantly highest contributions in *Sporobolus* and in mudflat habitats (Table 1). The highest contributions of colloidal carbohydrate to TOC were in upper salt marsh and channel habitats (1–2%), with the lowest contribution (0.32% of TOC) in MF sediment (Table 1). The contribution of BMA-carbon to sediment TOC was between 1.27% and 7.95% of sediment TOC in

Fig. 2. (**a**, **c**, **e**) Boxplots of sediment Chl *a*, colloidal carbohydrate and total carbohydrate content, in top 5 mm of sediment at different sites (*see* Supporting Information Table S1) in the North Inlet Estuary, S.C. in 2018 and 2023 ($n = 10$ except $n = 40$ for OLC18), mean value indicated by point; (**b**, **d**, **f**) vertical profiles from 5 sites, in surface (s) = 0–5 mm, middle (m) = 45–50 mm and bottom (b) 95–100 mm slices of 10 cm long sediment cores, $n = 3$ for each site, number = core number identifier.

the six different habitat types of the NEI. The highest relative contributions of BMA-carbon to sediment %TOC were in the habitats with lower overall %TOC (USM, ChS, ChM) and lowest in those habitats (SpT, SpS, MF) where other organic carbon sources predominate (Table 1).

Principal components analysis of Near-infrared (NIR) spectra separated sediments into two habitat-related groupings on PC1 (Supporting Information Fig. S7a). Upper salt marsh PC1 scores had a significant negative relationship with %TOC ($p < 0.001$) (Supporting Information Fig. S7b) while PC1 sample scores from SpS, SpT, and MF habitats were significantly positively related to sediment %TOC (Supporting Information Fig. S7b). Similar habitat differences were observed between NIR PC1 scores and other measures of sediment properties and BMA biofilm presence (Supporting Information Fig. S8).

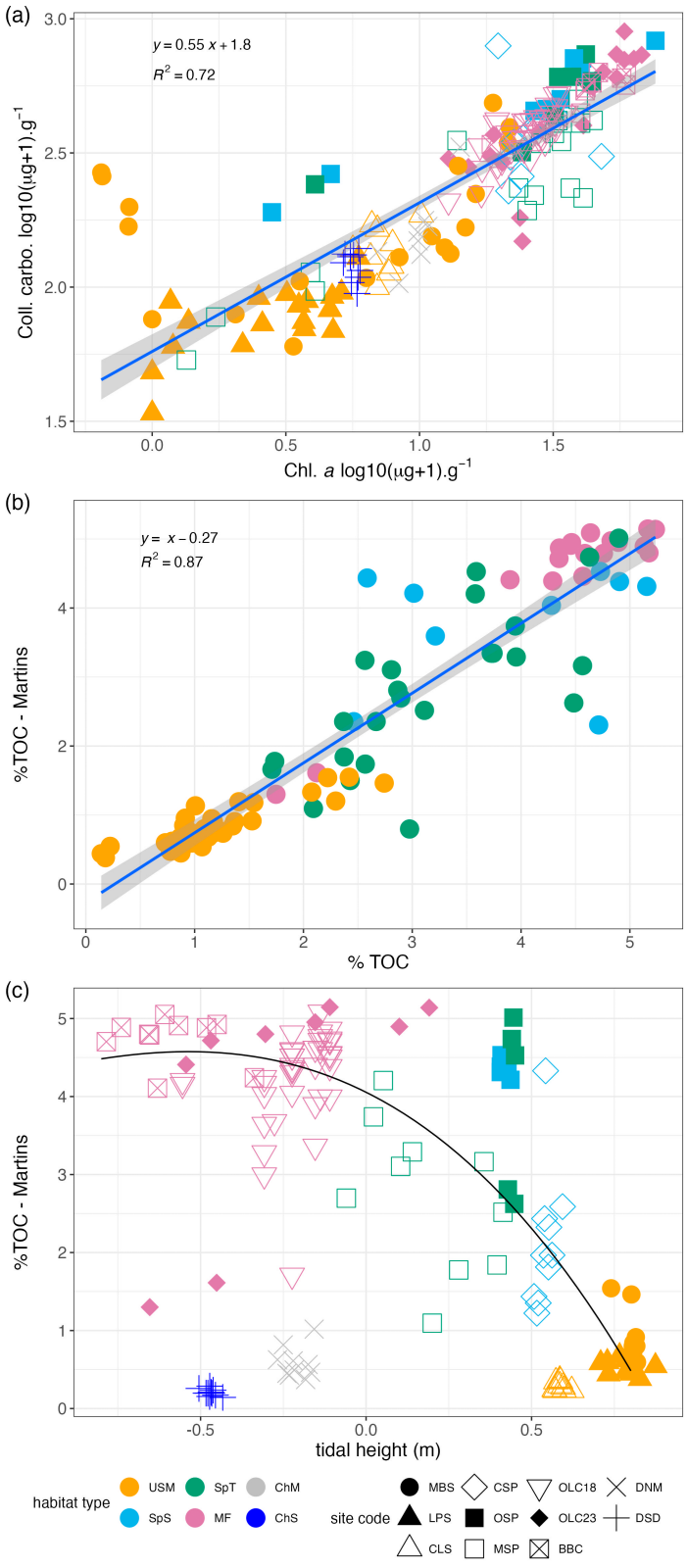

Deriving the marsh-scale total organic carbon stocks

Total sediment organic carbon stock (g C m^{-2} to a depth of 5 mm) was calculated for each 1 m^2 "pixel" of the LIDAR data of the NIE, considering %TOC and sediment bulk density data (Supporting Information Methods). TOC stock in the top 5 mm of sediment ranged from 1 to 115 g C m^{-2} (Supporting Information Fig. S9a). Given that total carbon and carbohydrate concentrations were the least affected by sampling depth (Fig. 2f), we assumed a constant distribution and bulk density over this distance and calculated carbon stocks (g C m^{-2} in the top 10 cm sediment) (Fig. 4a,b; Supporting Information Fig. S9b). Highest TOC stocks (1500–2000 g C m^{-2}) were present in the *Sporobolus* and mudflat habitats, with upper salt marsh habitats significantly lower (< 1000 g C m^{-2}). Benthic microalgal contributions to sediment TOC stocks were estimated using a similar approach. Values for BMA organic carbon (Table 1) were used to determine BMA organic carbon (g C m^{-2}) in the top 5 mm of sediment. Given the steep decreases in sediment colloidal carbohydrate and sediment Chl. *a* at greater depths (Fig. 2d), these values were scaled to a depth of 2.5 cm to avoid over-estimation of stock. Highest BMA organic carbon occurred in unvegetated upper salt marsh sediments and along mudflat creek edges (Fig. 4c). TOC and BMA carbon stock estimates were scaled up from m^2 to hectare-sized grids, generating a map of organic carbon stocks across the North Inlet Estuary (NIE). Values ranged from 0.0 to 21.0 t C ha^{-1} depending on the composition of the habitat within each hectare quadrat (Fig. 5a). Across the NIE salt marsh, organic carbon stocks per hectare were heterogeneous,

Fig. 3. (**a**) Relationship between $\log_{10}$ $(n + 1)$ sediment Chl. *a* and colloidal carbohydrate content (μg g^{-1}) across all sites and habitat types in the top 5 mm of sediment in North Inlet Estuary, S.C., in 2018 and 2023. Individual habitat regression parameters given in Supporting Information Table S2; (**b**) modeled sediment total organic carbon (%TOC) content (derived from %LOI using Martins et al. 2022) compared to actual %TOC values in 2023 dataset; (**c**) relationship between sediment tidal height (from LIDAR) and modeled %TOC for sites and habitat types. The polynomial best fit line ($r^2 = 0.73$, $p < 0.001$) is based on the in-marsh locations only (excluding DNM and DSD and three outlier OLC samples with very low estimated %TOC).

Table 1. Contribution of total carbohydrate, colloidal carbohydrate, and benthic microalgal (BMA) carbon (%) of the total organic carbon content of surface sediment (5 mm) in different habitats in the North Inlet Estuary, S.C. Carbohydrate contents calculated as μg C g^{-1} dry weight sediment and expressed as the percentage contribution to the total organic carbon (TOC) content (% dry weight) of sediments. BMA contribution, see text. TOC content derived from %LOI data, using Martins et al. 2022 model. Mean values with different superscripts are significantly different (ANOVA, $p < 0.05$ or less). s.d. = standard deviation.

Habitat type	Sediment TOC (% dw) mean ± s.d.	Total carbo. contrib. (%) to TOC mean ± s.d.	Colloidal carbo. contrib. (%) to TOC. Mean ± s.d.	BMA contrib. (%) to TOC mean ± s.d.	*n*
USM	$0.57^{A,E} \pm 0.32$	$13.5^{A} \pm 8.19$	$1.01^{A} \pm 0.60$	$3.91^{A} \pm 2.29$	30
SpS	$2.89^{B} \pm 1.31$	$23.3^{B} \pm 11.7$	$0.64^{B} \pm 0.41$	$2.45^{B} \pm 1.57$	15
SpT	$3.14^{B} \pm 1.14$	$19.8^{B} \pm 7.91$	$0.45^{B} \pm 0.13$	$1.77^{B} \pm 0.49$	15
MF	$4.31^{C} \pm 0.80$	$13.9^{C} \pm 3.04$	$0.32^{C} \pm 0.07$	$1.27^{C} \pm 0.27$	60
ChS	$0.58^{D,E} \pm 0.2$	$9.3^{A} \pm 3.23$	$1.08^{A} \pm 0.33$	$4.18^{A} \pm 1.28$	10
ChM	$0.21^{F} \pm 0.05$	$8.2^{D} \pm 2.21$	$2.06^{D} \pm 0.62$	$7.95^{D} \pm 2.38$	10

with the most frequent value between 14 and 16 t C ha^{-1} in the top 10 cm of sediment. Some of the highest sediment TOC stocks were present around the interfaces between areas of short *Sporobolus* (SpS) and upper salt marsh (USM) (Fig. 5a). BMA organic carbon stocks showed similar patterns of distribution with the median BMA carbon stock between 0.06 and 0.08 t C ha^{-1} and highest values (0.173 t C ha^{-1}) in regions of salt marsh containing large areas of unvegetated upper salt marsh sediments (Fig. 5b).

Discussion

In this study, we investigated the relationships between BMA biomass and sediment organic carbon content across a range of habitats and sediment types within a well-characterized Atlantic Coast North American salt marsh ecosystem. Using those data, we estimated the contribution of BMA carbon to the TOC stocks within salt marsh habitats and scaled those estimates to hectares and whole marsh areas.

Comparisons of BMA biomass and composition across the habitat types

Chlorophyll *a* is an established indirect measure for BMA biomass (Nedwell et al. 2016; Pinckney 2018), and the Chl. *a* content in different habitats reported here agrees with previous studies in US salt marsh environments, both in the NIE (Pinckney and Zingmark 1993a, 1993b, 1993c; Thornton et al. 2010) and in other locations (Thornton and Visser 2009; Plante et al. 2020). indicating a relatively stable pattern of inter-habitat differences. Sampling to a depth of 5 mm (similar to Plante et al. 2020; Thornton and Visser 2009; Thornton et al. 2010) may underestimate the high surface Chl. *a* concentrations resulting from vertical migration of BMA into the narrow photic zone of intertidal sediments (Pinckney and Zingmark 1991; Pinckney et al. 1994; Underwood et al. 2022). The depth of the photic zone varies with sediment properties and can extend to 1–3 mm or deeper (Pinckney and Zingmark 1993a; Jesus et al. 2009; Morelle et al. 2020). Normalizing to 5 mm deep and expressing data at mg Chl. *a* m^{-2} still revealed inter-habitat differences. The hydrodynamically active channel sites had the lowest Chl. *a* content, as continuous sediment disturbance redistributes BMA cells within the sediment profile and reduces surface accumulations of epipelic taxa (Hope et al. 2020; Underwood et al. 2022). Negligible Chl. *a* concentrations measured at 5 cm and 10 cm depths suggest that most of the active BMA are present in the top 5 mm of the sediment.

Diatoms were the predominant algal group across all habitats studied, consistent with previous findings in the NIE (Pinckney and Zingmark 1993b; Thornton et al. 2010). Sediment in the mudflat and *Sporobolus* habitats contains a high percentage of silts and clays (Pinckney and Zingmark 1993a), which favor epipelic diatoms and highly motile euglenids (Underwood et al. 2022). High de-epoxidation ratios indicate that BMA in these habitats were utilizing non-photosynthetic quenching (NPQ) coupled with micromigration, as a photoprotective strategy to maintain high rates of photosynthesis (Pinckney and Zingmark 1993a; Jesus et al. 2009; Cartaxana et al. 2016; Blommaert et al. 2018). *Sporobolus* stands create shade on the sediment surface (Pinckney and Zingmark 1993b), which can reduce rates of net BMA primary production compared to open mudflats (Pinckney and Zingmark 1993a) but also provides some protection from sediment resuspension (Kwon et al. 2020).

In the upper salt marsh sediments, BMA biomass was lower. BMA in these habitats is subject to a combination of desiccation stress, high temperatures, deeper light penetration (2–5 mm), and grazing and bioturbation by fiddler crabs (Pinckney 2023). The upper salt marsh BMA had the highest contribution of cyanobacteria, which are more tolerant of light and desiccation stresses (Bellinger et al. 2005; Cartaxana et al. 2016; Underwood et al. 2022). Despite pressures such as desiccation and grazing, an active BMA assemblage persisted in USM habitats, contributing to carbon cycling in these

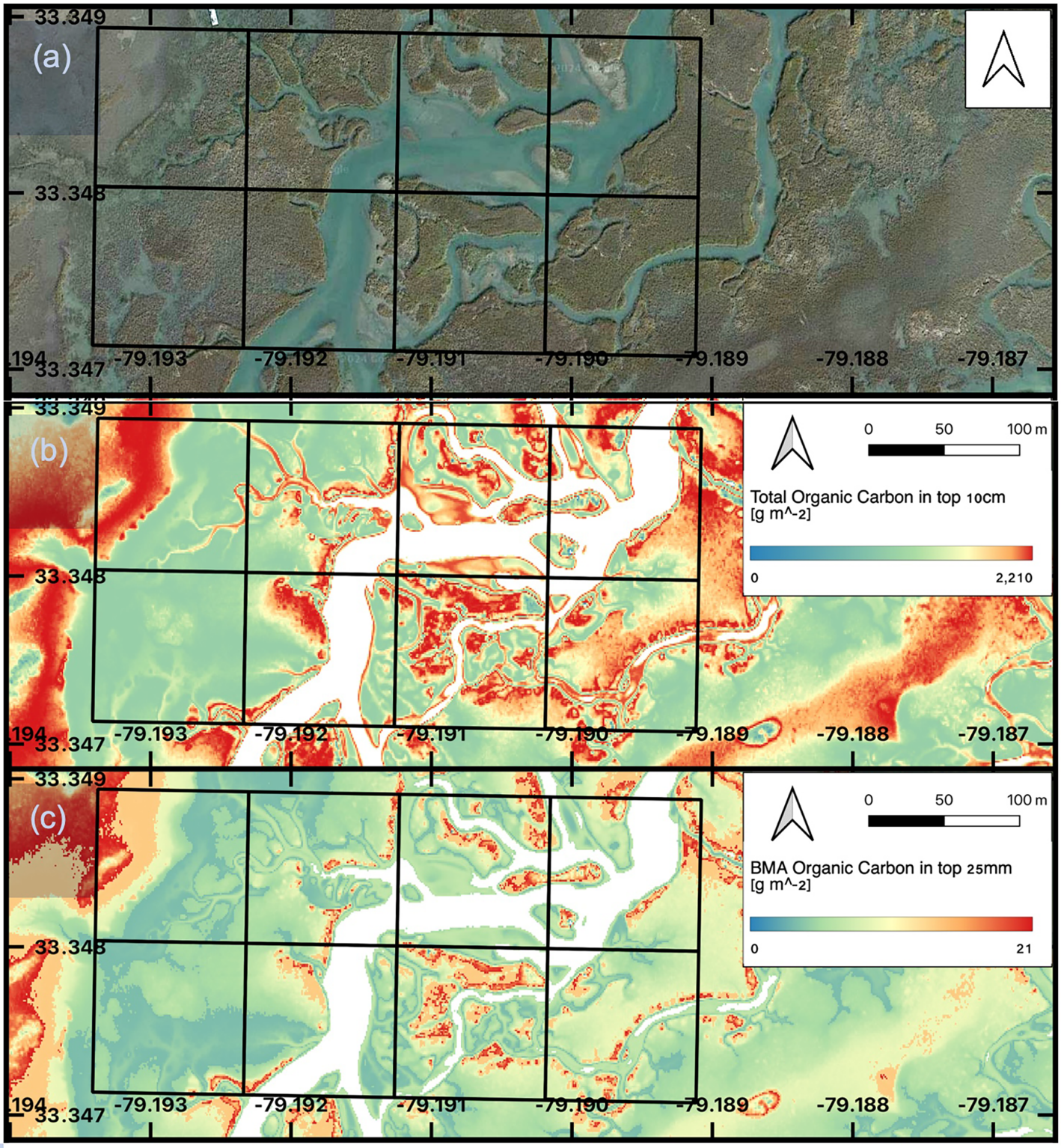

Fig. 4. (**a**) satellite image (Google Earth 2024); (**b**) high-resolution mapping (each pixel approx. 1 m^{-2}) of sediment TOC (g TOC m^{-2} in top 10 cm of sediment profile); and (**c**) BMA total organic carbon stocks (g TOC m^{-2} to a depth of 25 mm) within the NIE, South Carolina, United States. The overlain grid shows eight individual 1-ha areas.

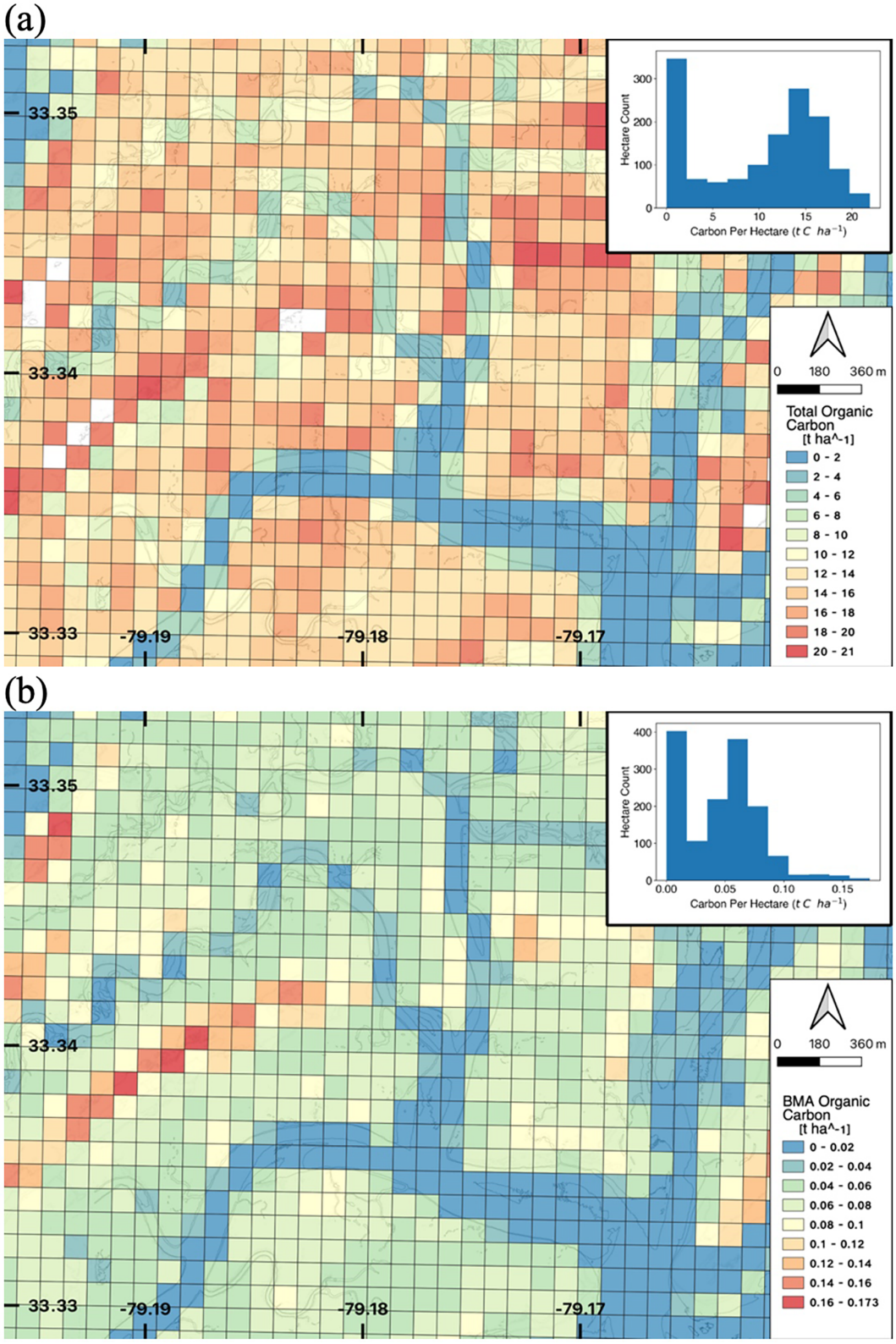

Fig. 5. (**a**) modeled sediment total organic carbon stocks (tons TOC in top 10 cm ha^{-1}) and (**b**) modeled BMA total organic carbon stocks (tons TOC in top 25 mm ha^{-1}) across the NIE, derived from NOAA height data and the relationships present in this paper. The mean value for each 1 ha square in (a) and (b) is based on the sum of the carbon values of the individual 1 m^2 habitat pixels present at that location (*see* Fig. 5). Insets, frequency distribution of TOC stock ha^{-1} values across the mapped area.

sediments. Intertidal sands have been characterized as low standing stock but high activity systems (Cook et al. 2007; Oakes et al. 2010, 2012; Frankenbach et al. 2019), with bioturbation by fiddler crabs enhancing sediment organic carbon cycling (Xiao et al. 2024).

Sampling in winter 2023 found strongly decreasing Chl. *a* and colloidal carbohydrate profiles with depth, agreeing with work showing decreases of 20–30% in Chl. *a* and total phaeopigments over 10 mm vertical profiles in NEI sediments (Pinckney and Zingmark 1993a; Pinckney et al. 1994), and in other BMA-dominated sediments (Jesus et al. 2006; Morelle et al. 2020). Colloidal carbohydrate concentrations are closely correlated with BMA biomass and productivity (Underwood 2024), and declines in colloidal carbohydrate with depth match previous work at both μm and mm scales (Taylor and Paterson 1998; Montani et al. 2003). Total carbohydrate measurements include detrital and other material (often termed bulk carbohydrates) from non-algal sources, as well as more refractory BMA-derived material (Bellinger et al. 2005; Bellinger et al. 2009), which explains the more homogenous vertical distribution profiles of total sediment carbohydrate down to 10 cm in the NIE sediment profiles.

BMA Chl. *a* and sediment carbohydrate relationships

Sediment colloidal carbohydrate content in marsh sediments was similar to previous measurements in the NIE (Thornton et al. 2010), though lower than in salt marshes in the Gulf of Mexico (Thornton and Visser 2009). Comparable colloidal carbohydrate concentrations have been measured in other temperate locations (Orvain et al. 2004; Bellinger et al. 2005; Redzuan and Underwood 2020; Hope et al. 2020). There were no significant differences between mudflat and *Sporobolus* habitats, indicating a minimal contribution of colloidal carbohydrates from halophyte material. In upper salt marsh sediment, colloidal carbohydrate concentrations were lower, a pattern observed in sandier unvegetated sediments elsewhere (Fiji, Underwood 2002; Australia, Oakes et al. 2010, 2012; U.K., Hope et al. 2020). Colloidal carbohydrate concentrations in intertidal sediments are closely coupled to BMA activity (Underwood et al. 2022; Underwood 2024). High Chl. *a*: Phaeo ratios and high proportions of colloidal carbohydrates in USM sites (Supporting Information Fig. S3a,b) indicate a high BMA activity despite lower concentrations. This suggests that the colloidal carbohydrate and sediment organic carbon in the upper salt marsh are more closely related to BMA primary production, rather than being diluted by high background concentrations of autochthonous and allochthonous detrital carbon components.

Colloidal carbohydrate concentrations were closely correlated with BMA biomass (Chl. *a*) across all six habitats studied in the NIE. Colloidal carbohydrate extractions predominantly measure microphytobenthic exudates: a combination of lower molecular weight sugars, polysaccharides, and extracellular polymeric substances (EPS, Underwood et al. 2022; Underwood 2024). Colloidal carbohydrates and EPS are important structural components of intertidal sediment biofilms, increasing sediment stability (Hope et al. 2020; Kim et al. 2021). Across the NIE marsh sites, the slope of the colloidal-Chl *a* relationship was 0.55, approximately half that of the Underwood and Smith (1998) model. This would suggest background contributions from other sources of carbohydrate in the marsh sediments, material not present in the tidally mixed lower shore sediments (e.g., channel sands; Supporting Information Table S3). Previous work reports significant correlations between sediment Chl. *a* and EPS and low-molecular-weight carbohydrates from mudflat sites close to Oyster Landing location (Thornton et al. 2010), between various carbohydrate fractions and sediment Chl. *a* content in salt marsh sediments in Texas (Thornton and Visser 2009), and elsewhere, with stronger relationships in muddier sediments (Orvain et al. 2004; Morelle et al. 2020). This reflects the greater relative importance of BMA contributions to sediment carbohydrate stocks in unvegetated sediments (Underwood 2002). The presence of clear relationships between BMA biomass (sediment Chl. *a*) and biofilm parameters (total, colloidal carbohydrate) across a range of habitats and sediment types provides a basis to consider the contribution of BMA to sediment organic stocks.

Sediment organic matter and organic carbon BMA contribution to the sediment carbon pool

The values for soil organic matter (SOM) reported here (2–18% within different habitats) agreed with previous work in the NIE of SOM between 18% and 30% LOI in *Sporobolus* beds, with lower values in unvegetated creek sediments (15% LOI) and 6.5% LOI at the seaward end of Debidue Creek (close to site ChS) (Wigand et al. 2015). SOM as high as 51% is reported in east coast US salt marshes, particularly in brackish water and swamp coastal marsh systems (Craft et al. 1988, 1991), while mesohaline and polyhaline *Sporobolus* marshes in North Carolina, USA, had SOM values between 1.2% and 23.5% (Craft et al. 1988). SOM values in the NIE are therefore lower than values reported for a wide range of salt marsh locations (Maxwell et al. 2023). This likely reflects the mineralogenic nature of the sediments and the polyhaline conditions across the NIE, compared to organogenic coastal and brackish marshes that have much higher sediment organic contents (Craft et al. 1991; van der Broek et al. 2018; Holmquist et al. 2018; Ouyang and Lee 2020; Maxwell et al. 2023).

There is significant interest in using %LOI as a proxy for sediment organic carbon content (Craft et al. 1991; Ouyang and Lee 2020; Maxwell et al. 2023), as elemental analysis is not always available. Applying Craft et al.'s (1991) model from North Carolina salt marshes and the global model of Maxwell et al. (2023) significantly overestimated %TOC when compared to the direct %TOC measurements made at our NIE sites. Applying these general models to marine-influenced coastal salt marshes thus overestimates the %TOC from the %

LOI data, as they include data from brackish and organogenic marshes, which have significantly higher SOM and TOC values (van der Broek et al. 2018; Maxwell et al. 2023). The model of Martins et al. (2022), based on a study of a Portuguese estuarine embayment, had a gradient fit of 1.0 with our 2023 %TOC data (Fig. 3b), with a ratio of %TOC/LOI of 0.35. Applying the Martins et al. (2022) model, derived sediment % TOC values ranged from 0.5% to 5%, in agreement with studies of similar coastal marshes in this region (Craft et al. 1988; Morris and Whiting 1986).

The contribution of BMA to sediment organic carbon stocks was calculated from our field data and various literature values (*see* Supporting Information Methods), giving estimates of the BMA organic carbon contribution of between 1.27% and 7.95% of the total sediment organic content (Table 1), with values between 1 and 27 g C m^2 when scaled to a depth of 2.5 cm. These values are close to previously published estimates of BMA carbon contribution in sediments, derived either by direct counts and biovolume estimates (0.26–3.3 g C m^{-2}; Sundbäck et al. 1996), or using Chl *a* to carbon conversion factors (between 1 and 4 g C m^{-2} but occasionally higher [20–30 g C m^{-2}]; Sündback and McGlathery 2005; Montani et al. 2003).

NIR spectra have been used to predict differences in total organic matter in mangrove and *Sporobolus* wetlands (Romero et al. 2017; Song et al. 2022). Differences in the NIR spectra of sediments from different habitats (Supporting Information Fig. S6) are related to SOM composition and concentration (Yang 2020; Song et al. 2022; Walden et al. 2024). In our study, the upper salt marsh showed an inverse relationship between spectra components and sediment organic carbon (% TOC) compared with the other habitats. This distinct spectral signal may relate to the greater contribution of BMA-derived organic carbon (Table 1; Supporting Information Fig. S4a,b) in this habitat. In *Sporobolus* and mudflat habitats, any BMA-related NIR signal would be masked due to the higher concentrations of detrital organic carbon present. There are other factors that covary with %TOC, such as particle size and mineralogy, that can influence NIR spectra (Yang 2020; Song et al. 2022). Therefore, further work is needed to understand the potential of NIR to detect SOM differences, which could serve as proxies for BMA contribution to sediment organic composition in the future.

Estimating contributions to marsh-scale carbon stocks

The zonation of habitats in the East Coast United States salt marshes is closely aligned with tidal height (Dame et al. 2000; Morris et al. 2005). Using our model, we were able to estimate organic carbon stocks at tidal heights between −0.78 and 0.98 m, capturing the majority of the salt marsh habitat (Morris et al. 2005). Hectare-scale estimates can rely on upscaling from limited numbers of sediment core samples collected across a highly heterogeneous landscape (Ladd et al. 2022). Our model, based on aggregating m^2 estimates, avoids that problem. Salt marsh carbon stocks are typically reported in tons (Mg) C ha^{-1} to a depth of 1 m, in line with IPCC recommendations (IPCC 2014). One approach is to extrapolate surface measurements to a 1 m depth, assuming an equal carbon stock profile, but this risks overestimating carbon stocks in salt marsh sediments (Mason et al. 2023; Maxwell et al. 2024). Other authors have restricted scaling to the top 10 cm or 30 cm of marsh sediment as stock profiles may exhibit significant diagenetic differences and even represent previous habitat types that have influenced the development of salt marshes (Ladd et al. 2022; Smeaton et al. 2023). Based on the relatively even %LOI and total carbohydrate content profiles we scaled to the top 10 cm. Similarly, given the absence of Chl. *a* in deeper samples, we only extrapolated the BMA contribution to the top 2.5 cm. We recommend limiting BMA carbon stock measurements to this depth, to avoid overestimation. This does not mean that no BMA carbon is present at greater depths, as more refractory diatom-derived EPS is only slowly degraded in deeper sediments (Bohórquez et al. 2017; Underwood et al. 2022). Thus, our total and BMA organic carbon stock estimates per ha are conservative.

We report median organic carbon stocks of 15 t C ha^{-1} and a median BMA carbon contribution of 0.06–0.08 t C ha^{-1}. These values are lower than global estimates based on extrapolation to a 1 m depth for salt marshes and intertidal mudflats (287 ± 238.64 t C ha^{-1} and 101.5 ± 11.4 t C ha^{-1}, respectively; Chen and Lee 2022; Mason et al. 2023). In 30 cm depth profiles, Morris and Whiting (1986) found homogeneity in SOM profiles in tall *Sporobolus* habitats, though 50% declines in %LOI in short *Sporobolus* sediments in the NIE, and Wigand et al. (2015) found no appreciable declines in total organic content in the top 30 cm of NIE sediments. Assuming similar homogeneity, our median TOC stock would be 45 t C h^{-1}, similar to values for temperate South American (43 t ha^{-1}; Martinetto et al. 2023) and European (40–60 t C ha^{-1}, Mazarrasa et al. 2023) salt marshes. A recent global analysis indicated that salt marshes of the Carolinas (United States) have 70–75 t organic C h^{-1} in the top 30 cm, though this includes brackish marshes with higher sediment organic matter content (Maxwell et al. 2024). The values we report here correspond to marine-influenced coastal salt marshes that fall in the lower end of global carbon estimates.

There is currently strong interest from policymakers, conservationists, and NGOs in exploring the role that salt marshes may play in climate mitigation (Preston et al. 2025). In our study, we have estimated conservative values for the contribution of benthic microalgal biofilms to salt marsh organic carbon stocks. The contribution of BMA biomass to the sediment carbon stock is around 10% of the annual BMA primary production (BMA annual net primary production in the NIE, 92–234 g C m^{-2} y^{-1}, Pinckney and Zingmark 1993b) and in other coastal habitats (Pinckney 2018; Underwood et al. 2022). This is not surprising, much BMA primary production is labile, and the majority of BMA fixed carbon is

utilized by microbes or consumed by animals (Pinckney 2018; Christianen et al. 2017; Kim et al. 2021; Underwood et al. 2022). Sediment carbon stocks are fixed amounts at a point in time, and such estimates do not account for the turnover of different organic carbon pools through which 100–250 g C m^{-2} per year of BMA primary production flows. The turnover of colloidal carbohydrate pools is rapid though there is greater uncertainty about the long-term fate of more refractory diatom EPS in sediment (Underwood 2002; Bellinger et al. 2009; Bohórquez et al. 2017). BMA may also indirectly facilitate increased saltmarsh carbon stocks through the stabilization of sediments and promotion of halophyte colonization (Nedwell et al. 2016; Hope et al. 2020). BMA are an important component in the regulation and turnover of carbon in salt marshes, and more work is required on their contribution to "blue carbon" sequestration.

Author Contributions

Graham J. C. Underwood: Conceptualization, funding acquisition, investigation, methodology, writing – original draft preparation, writing – review and editing. **Nicola J. D. Slee:** Investigation, methodology writing – review and editing. **Jessica C. J. Underwood:** Investigation, methodology, formal analysis, writing – review and editing. **Christopher I. D. Underwood:** Investigation, methodology, formal analysis, software and visualization, writing – review and editing; **James L. Pinckney:** Conceptualization, funding acquisition, methodology, writing – review and editing.

Acknowledgments

We thank Jessica Hardy for laboratory sample analysis, Matt Kimball for field site logistics, and two anonymous reviewers for their helpful comments. This study was funded by the U.K. Royal Society (IES\R1\201260) to Graham J. C. Underwood, Nicola J. D. Slee, and James L. Pinckney, a Visiting Scientist Award to Graham J. C. Underwood from the University of South Carolina's Baruch Marine Field Laboratory (BMFL), UKRI NERC, award NE/V01868X/1 to Graham J. C. Underwood, and partial funding (James L. Pinckney) for this project was supplied by the U.S. National Science Foundation (OCE 2241830).

Conflicts of Interest

None declared.

Data Availability Statement

Data available on request from the authors.

References

Adams, J. B. 2020. "Salt Marsh at the Tip of Africa: Patterns, Processes and Changes in Response to Climate Change." *Estuarine, Coastal and Shelf Science* 237: 106650. https://doi.org/10.1016/j.ecss.2020.106650.

Allen, D. M., W. B. Allen, R. F. Feller, and J. S. Plunket, eds. 2014. Site Profile of the North Inlet—Winyah Bay National Estuarine Research Reserve, 432. Georgetown, SC: North Inlet—Winyah Bay National Estuarine Research Reserve.

Aslam, S. N., T. Cresswell-Maynard, D. N. Thomas, and G. J. C. Underwood. 2012. "Production and Characterisation of the Intra- and Extracellular Carbohydrates and Polymeric Substances (EPS) of Three Sea Ice Diatom Species, and Evidence for a Cryoprotective Role for EPS." *Journal of Phycology* 48: 1494–1509. https://doi.org/10.1111/jpy.12004.

Bellinger, B. J., A. S. Abdullahi, M. R. Gretz, and G. J. C. Underwood. 2005. "Biofilm Polymers: Relationship Between Carbohydrate Biopolymers From Estuarine Mudflats and Unialgal Cultures of Benthic Diatoms." *Aquatic Microbial Ecology* 38: 169–180. https://doi.org/10.3354/ame038169.

Bellinger, B. J., G. J. C. Underwood, S. E. Ziegler, and M. R. Gretz. 2009. "Significance of Diatom-Derived Polymers in Carbon Flow Dynamics Within Estuarine Biofilms Determined Through Isotopic Enrichment." *Aquatic Microbial Ecology* 55: 169–187. https://doi.org/10.3354/ame01287.

Blommaert, L., J. Lavaud, W. Vyverman, and K. Sabbe. 2018. "Behavioural Versus Physiological Photoprotection in Epipelic and Epipsammic Benthic Diatoms." *European Journal of Phycology* 53: 146–155. https://doi.org/10.1080/09670262.2017.1397197.

Bohórquez, J., T. J. McGenity, S. Papaspyrou, E. García-Robledo, A. Corzo, and G. J. C. Underwood. 2017. "Different Types of Diatom-Derived Extracellular Polymeric Substances Drive Changes in Heterotrophic Bacterial Communities From Intertidal Sediments." *Frontiers in Microbiology* 8: 245. https://doi.org/10.3389/fmicb.2017.00245.

Cahoon, L. B. 1999. "The Role of Benthic Microalgae in Neritic Ecosystems." *Oceanography and Marine Biology: An Annual Review* 37: 47–86. https://doi.org/10.1201/9781482298550.

Cartaxana, P., L. Ribeiro, J. W. Goessling, S. Cruz, and M. Kühl. 2016. "Light and O_2 Microenvironments in Two Contrasting Diatom-Dominated Coastal Sediments." *Marine Ecology Progress Series* 545: 35–47. https://doi.org/10.3354/meps11630.

Chen, Z. L. and S. Y. Lee. 2022. "Tidal Flats as a Significant Carbon Reservoir in Global Coastal Ecosystems." *Frontiers in Marine Science* 9: 900896. https://doi.org/10.3389/fmars.2022.900896.

Christianen, M. J. A., J. J. Middleburg, S. J. Holthusijsen, et al. 2017. "Benthic Primary Producers Are Key to Sustain the Wadden Sea Food Web: Stable Carbon Isotope Analysis at Landscape Scale." *Ecology* 98: 1498–1512. https://doi.org/10.1002/ecy.1837.

Cibic, T., S. Fazi, F. Nasi, et al. 2019. "Natural and Anthropogenic Disturbances Shape Benthic Phototrophic and Heterotrophic Microbial Communities in the Po River Delta System." *Estuarine, Coastal and Shelf Science* 222: 168–182. https://doi.org/10.1016/j.ecss.2019.04.009.

Cook, P. L. M., B. Veuger, S. Boer, and J. J. Middelburg. 2007. "Effect of Nutrient Availability on Carbon and Nitrogen Incorporation and Flows Through Benthic Algae and Bacteria in near-Shore Sandy Sediment." *Aquatic Microbial Ecology* 49: 165–180. https://doi.org/10.3354/ame01142.

Craft, C. B., S. W. Broome, and E. D. Seneca. 1988. "Nitrogen, Phosphorus and Organic Carbon Pools in Natural and Transplanted Marsh Soils." *Estuaries* 11: 272–280. https://doi.org/10.2307/1352014.

Craft, C. B., E. D. Seneca, and S. W. Broome. 1991. "Loss on Ignition and Kjeldahl Digestion for Estimating Organic Carbon and Total Nitrogen in Estuarine Marsh Soils: Calibration With Dry Combustion." *Estuaries* 14: 175–179. https://doi.org/10.2307/1351691.

Dame, R., M. Alber, D. Allen, et al. 2000. "Estuaries of the South Atlantic Coast of North America: Their Geographical Signatures." *Estuaries* 23: 793–819. https://doi.org/10.2307/1352999.

Frankenbach, S., A. A. Azevedo, V. Reis, et al. 2019. "Functional Resilience of PSII, Vertical Distribution and Ecosystem-Level Estimates of Subsurface Microphytobenthos in Estuarine Tidal Flats." *Continental Shelf Research* 182: 46–56. https://doi.org/10.1016/j.csr.2019.05.018.

Frankenbach, S., J. Ezequiel, S. Plecha, et al. 2020. "Synoptic Spatio-Temporal Variability of the Photosynthetic Productivity of Microphytobenthos and Phytoplankton in a Tidal Estuary." *Frontiers in Marine Science* 7: 170. https://doi.org/10.3389/fmars.2020.00170.

Hardison, A. K., E. A. Canuel, I. C. Anderson, C. R. Tobias, B. Veuger, and M. N. Waters. 2013. "Microphytobenthos and Benthic Macroalgae Determine Sediment Organic Matter Composition in Shallow Photic Sediments." *Biogeosciences* 10: 5571–5588. https://doi.org/10.5194/bg-10-5571-2013.

Haro, S., M. Lara, I. Laiz, et al. 2020. "Microbenthic Net Metabolism Along Intertidal Gradients (Cadiz Bay, SW Spain): Spatio-Temporal Patterns and Environmental Factors." *Frontiers in Marine Science* 7: 39. https://doi.org/10.3389/fmars.2020.00039.

Higgins, H., S. Wright, and L. Schlüter. 2011. "Quantitative Interpretation of Chemotaxonomic Pigment Data." In Phytoplankton Pigments, edited by S. Roy, C. A. Llewellyn, E. S. Egeland, and G. Johnsen. NY: Cambridge University Press.

Holmquist, J. R., L. Windham-Myers, N. Bliss, et al. 2018. "Accuracy and Precision of Tidal Wetland Soil Carbon Mapping in the Conterminous United States." *Science Reports* 8: 9478. https://doi.org/10.1038/s41598-018-26948-7.

Hope, J. A., J. Malarkey, J. H. Baas, et al. 2020. "Interactions Between Sediment Microbial Ecology and Physical Dynamics Drive Heterogeneity in Contextually Similar Depositional Systems." *Limnology and Oceanography* 65: 2403–2419. https://doi.org/10.1002/lno.11461.

IPCC. 2014. 2013 Supplement to the 2006 IPCC Guidelines for National Greenhouse Gas Inventories: Wetlands, edited by T. Hiraishi, T. Krug, K. Tanabe, et al. IPCC.

Jesus, B., V. Brotas, L. Ribeiro, C. R. Mendes, P. Cartaxana, and D. M. Paterson. 2009. "Adaptations of Microphytobenthos Assemblages to Sediment Type and Tidal Position." *Continental Shelf Research* 29: 1624–1634. https://doi.org/10.1016/j.csr.2009.05.006.

Jesus, B., C. R. Mendes, V. Brotas, and D. M. Paterson. 2006. "Effect of Sediment Type on Microphytobenthos Vertical Distribution: Modelling the Productive Biomass and Improving Ground Truth Measurements." *Journal of Experimental Marine Biology and Ecology* 332: 60–74. https://doi.org/10.1016/j.jembe.2005.11.005.

Kim, B., J. Lee, J. Noh, et al. 2021. "Spatiotemporal Variation of Extracellular Polymeric Substances (EPS) Associated With the Microphytobenthos of Tidal Flats in the Yellow Sea." *Marine Pollution Bulletin* 171: 112780. https://doi.org/10.1016/j.marpolbul.2021.112780.

Kwon, B.-O., H. Kim, J. Noh, S. Y. Lee, J. Nam, and J. S. Khim. 2020. "Spatiotemporal Variability in Microphytobenthic Primary Production Across Bare Intertidal Flat, Saltmarsh, and Mangrove Forest of Asia and Australia." *Marine Pollution Bulletin* 151: 110707. https://doi.org/10.1016/j.marpolbul.2019.110707.

Ladd, C. J., C. Smeaton, M. W. Skov, and W. E. Austin. 2022. "Best Practice for Upscaling Soil Organic Carbon Stocks in Salt Marshes." *Geoderma* 428: 116188. https://doi.org/10.1016/j.geoderma.2022.116188.

Ladd, C. J. T., M. F. Duggan-Edwards, T. J. Bouma, J. F. Pagès, and M. W. Skov. 2019. "Sediment Supply Explains Long-Term and Large-Scale Patterns in Salt Marsh Lateral Expansion and Erosion." *Geophysical Research Letters* 46: 11178–11187. https://doi.org/10.1029/2019GL083315.

Martinetto, P., J. Alberti, M. E. Becherucci, et al. 2023. "The Blue Carbon of Southern Southwest Atlantic Salt Marshes and Their Biotic and Abiotic Drivers." *Nature Communications* 14: 8500. https://doi.org/10.1038/s41467-023-44196-w.

Martins, M., C. B. de los Santos, P. Masque, R. A. Carrasco, C. Veiga-Pires, and R. Santos. 2022. "Carbon and Nitrogen Stocks and Burial Rates in Intertidal Vegetated Habitats of a Mesotidal Coastal Lagoon." *Ecosystems* 25: 372–386. https://doi.org/10.1007/s10021-021-00660-6.

Mason, V. G., A. Burden, G. Epstein, L. L. Jupe, K. A. Wood, and M. W. Skov. 2023. "Blue Carbon Benefits From Global Saltmarsh Restoration." *Global Change Biology* 29: 6517–6545. https://doi.org/10.1111/gcb.16943.

Maxwell, T. L., A. S. Rovai, and M. F. Adame. 2023. "Global Dataset of Soil Organic Carbon in Tidal Marshes." *Scientific Data* 10: 797. https://doi.org/10.1038/s41597-023-02633-x.

Maxwell, T. L., M. D. Spalding, D. A. Friess, et al. 2024. "Soil Carbon in the World's Tidal Marshes." *Nature Communications* 15: 10265. https://doi.org/10.1038/s41467-024-54572-9.

Mazarrasa, I., J. M. Neto, T. J. Bouma, et al. 2023. "Drivers of Variability in Blue Carbon Stocks and Burial Rates Across

European Estuarine Habitats." *Science of the Total Environment* 886: 163957. https://doi.org/10.1016/j.scitotenv.2023.163957.

McKew, B. A., A. Dumbrell, J. D. Taylor, T. J. McGenity, and G. J. C. Underwood. 2013. "Differences Between Aerobic and Anaerobic Degradation of Microphytobenthic Biofilm-Derived Organic Matter Within Intertidal Sediments." *FEMS Microbiology Ecology* 84: 495–509. https://doi.org/10.1111/1574-6941.12077.

Montani, S., P. Magni, and N. Abe. 2003. "Seasonal and Interannual Patterns of Intertidal Microphytobenthos in Combination With Laboratory and Areal Production Estimates." *Marine Ecology Progress Series* 249: 79–91. https://doi.org/10.3354/meps249079.

Morelle, J., P. Claquin, and F. Orvain. 2020. "Evidence for Better Microphytobenthos Dynamics in Mixed Sand/Mud Zones That in Pure Sand or Mud Intertidal Flats (Seine Esuary, Normandy, France)." *PLoS One* 15: e0237211. https://doi.org/10.1371/journal.pone.0237211.

Morris, J. T., D. Porter, M. Neet, et al. 2005. "Integrating LIDAR Elevation Data, Multi-Spectral Imagery and Neural Network Modelling for Marsh Characterization." *International Journal of Remote Sensing* 26: 5221–5234. https://doi.org/10.1080/01431160500219018.

Morris, J. T., and G. J. Whiting. 1986. "Emission of Gaseous Carbon Dioxide From Salt-Marsh Sediments and Its Relation to Other Carbon Losses." *Estuaries* 9: 9–19. https://doi.org/10.2307/1352188.

Nedwell, D. B., G. J. C. Underwood, T. J. McGenity, C. Whitby, and A. J. Dumbrell. 2016. "The Colne Estuary: A Long-Term Microbial Ecology Observatory." *Advances in Ecological Research* 55: 227–281. https://doi.org/10.1016/bs.aecr.2016.08.004.

Oakes, J. M., and B. D. Eyre. 2014. "Transformation and Fate of Microphytobenthos Carbon in Subtropical, Intertidal Sediments: Potential for Long-Term Carbon Retention Revealed by ^{13}C-Labeling." *Biogeosciences* 11: 1927–1940. https://doi.org/10.5194/bg-11-1927-2014.

Oakes, J. M., B. D. Eyre, and J. J. Middelburg. 2012. "Transformation and Fate of Microphytobenthos Carbon in Subtropical Shallow Subtidal Sands: A ^{13}C-Labeling Study." *Limnology and Oceanography* 57: 1846–1856. https://doi.org/10.4319/lo.2012.57.6.1846.

Oakes, J. M., B. D. Eyre, J. J. Middelburg, and H. T. S. Boschker. 2010. "Composition, Production, and Loss of Carbohydrates in Subtropical Shallow Subtidal Sandy Sediments: Rapid Processing and Long-Term Retention Revealed by ^{13}C-Labeling." *Limnology and Oceanography* 55: 2126–2138. https://doi.org/10.4319/lo.2010.55.5.2126.

Orvain, F., P. G. Sauriau, A. Sygut, L. Joassard, and P. Le Hir. 2004. "Interacting Effects of Hydrobia Ulvae Bioturbation and Microphytobenthos on the Erodibility of Mudflat Sediments." *Marine Ecology Progress Series* 278: 205–223. https://doi.org/10.3354/meps278205.

Ouyang, X., and S. Y. Lee. 2020. "Improved Estimates on Global Carbon Stock and Carbon Pools in Tidal Wetlands." *Nature Communications* 11: 317. https://doi.org/10.1038/s41467-019-14120-2.

Pinckney, J. L. 2018. "A Mini-Review of the Contribution of Benthic Microalgae to the Ecology of the Continental Shelf in the South Atlantic Bight." *Estuaries and Coasts* 41: 2070–2078. https://doi.org/10.1007/s12237-018-0401-z.

Pinckney, J. L. 2023. "Benthic Microaglal Community Structure, Primary Productivity, and Fiddler Crab (*Leptuca pugilator*) Grazing in an Estuarine Salt Panne." *Estuaries and Coasts* 46: 1316–1325. https://doi.org/10.1007/s12237-023-01208-8.

Pinckney, J. L., Y. Piceno, and C. Lovell. 1994. "Short-Term Changes in the Vertical Distribution of Benthic Microalgal Biomass in Intertidal, Muddy Sediments." *Diatom Research* 9: 143–153. https://doi.org/10.1080/0269249X.1994.9705293.

Pinckney, J. L., and R. G. Zingmark. 1991. "The Effects of Tidal Stage and Sun Angles on Intertidal Benthic Microalgal Productivity." *Marine Ecology Progress Series* 76: 81–89. https://doi.org/10.3354/meps076081.

Pinckney, J. L., and R. G. Zingmark. 1993*a*. "Biomass and Production of Benthic Microalgal Communities in Estuarine Habitats." *Estuaries* 16: 667–897. https://doi.org/10.2307/1352447.

Pinckney, J. L., and R. G. Zingmark. 1993*b*. "Modelling the Annual Production of Intertidal Benthic Microalgae in Estuarine Ecosystems." *Journal of Phycology* 29: 396–407. https://doi.org/10.1111/j.1529-8817.1993.tb00140.x.

Pinckney, J. L., and R. G. Zingmark. 1993*c*. "Photophysiological Responses of Intertidal Benthic Microalgal Communities to In Situ Light Environments: Methodological Considerations." *Limnology and Oceanography* 38: 1373–1383. https://doi.org/10.4319/lo.1993.38.7.1373.

Plante, C. J., K. Hill-Spanik, M. Cook, and C. Graham. 2020. "Environmental and Spatial Influences on Biogeography and Community Structure of Saltmarsh Benthic." *Estuaries and Coasts* 44: 147–161. https://doi.org/10.1007/s12237-020-00779-0.

Preston, J., A. Debney, C. Gamble, et al. 2025. "Seascape Connectivity: Evidence, Knowledge Gaps and Implications for Temperate Coastal Ecosystem Restoration Practice and Policy." *npj Ocean Sustainability* 4, no. 1: 33. https://doi.org/10.1038/s44183-025-00128-3.

R Core Team. 2024. "*Pile of Leaves*." The R Foundation for Statistical Computing Platform: aarch64-apple-darwin20. R Version 4.4.2.

Redzuan, N. S., and G. J. C. Underwood. 2020. "Movement of Microphytobenthos and Sediment Between Mudflats and Salt Marsh During Spring Tides." *Frontiers in Marine Science* 7: 496. https://doi.org/10.3389/fmars.2020.00496.

Romero, D. J., G. N. Nóbrega, X. L. Otero, and T. O. Ferreira. 2017. "Diffuse Reflectance Spectroscopy (Vis-Nir-Swir) as a

Promising Tool for Blue Carbon Quantification in Mangrove Soils: A Case of Study in Tropical Semiarid Climatic Conditions." *Soil Science Society of America Journal* 81: 1661–1667. https://doi.org/10.2136/sssaj2017.04.0135.

Smeaton, C., L. McMahon, E. Garrett, et al. 2023. "Organic Carbon Stocks of Great British Saltmarshes." *Frontiers in Marine Science* 10: 1229486. https://doi.org/10.3389/fmars.2023.1229486.

Song, J., J. Gao, Y. Zhang, et al. 2022. "Estimation of Soil Organic Carbon Content in Coastal Wetlands With Measured VIS-NIR Spectroscopy Using Optimized Support Vector Machines and Random Forests." *Remote Sensing* 14: 4372. https://doi.org/10.3390/rs14174372.

Stal, L. J., H. Vangemerden, and W. E. Krumbein. 1984. "The Simultaneous Assay of Chlorophyll and Bacteriochlorophyll in Natural Microbial Communities." *Journal of Microbiological Methods* 2: 295–306. https://doi.org/10.1016/0167-7012(84)90048-4.

Sundbäck, K., C. Nilsson, S. Odmark, and A. Wulff. 1996. "Does Ambient UV-B Radiation Influence Marine Diatom-Dominated Microbial Mats ? A Case Study." *Aquatic Microbial Ecology* 11: 151–159. https://doi.org/10.3354/ame011151.

Sündback, K., and K. McGlathery. 2005. "Interactions Between Benthic Macroalgal and Microalgal Mats." *Coastal and Estuarine Studies* 60: 7–29. https://doi.org/10.1029/CE060p0007.

Taylor, I. S., and D. M. Paterson. 1998. "Microspatial Variation in Carbohydrate Concentrations With Depth in the Upper Millimetres of Intertidal Cohesive Sediments." *Estuarine, Coastal and Shelf Science* 46: 359–370. https://doi.org/10.1006/ecss.1997.0288.

Thornton, D. C. O., S. M. Kopac, and R. A. Long. 2010. "Production and Enzymatic Hydrolysis of Carbohydrates in Intertidal Sediment." *Aquatic Microbial Ecology* 60: 109–125. https://doi.org/10.3354/ame01403.

Thornton, D. C. O., and L. A. Visser. 2009. "Measurement of Acid Polysaccharides (APS) Associated With Microphytobenthos in Salt Marsh Sediments." *Aquatic Microbial Ecology* 54: 185–198. https://doi.org/10.3354/ame01265.

Underwood, G. J. C. 2002. "Adaptations of Tropical Marine Microphytobenthic Assemblages Along a Gradient of Light and Nutrient Availablilty in Suva Lagoon, Fiji." *European Journal of Phycology* 37: 449–462. https://doi.org/10.1017/S0967026202003785.

Underwood, G. J. C. 2024. "Extracellular Polymeric Substance Production by Benthic Pennate Diatoms, Chapter 10." In Diatom Photosynthesis: From Primary Production to High-Value Molecules, edited by J. W. Goessling, J. Serôdio, and J. Lavaud, 303–326. Scrivener Publishing LLC.

Underwood, G. J. C., A. J. Dumbrell, T. J. McGenity, B. A. McKew, and C. Whitby. 2022. "The Microbiome of Coastal Sediments. Chapter 12." In The Marine Microbiome, edited by L. J. Stal and S. Cretoiu. Springer Nature Switzerland AG.

Underwood, G. J. C., and D. J. Smith. 1998. "Predicting Epipelic Diatom Exopolymer Concentrations in Intertidal Sediments from Sediment Chl. *a*." *Microbial Ecology* 35: 116–125. https://doi.org/10.1007/s002489900066.

van der Broek, M., C. Vandendriessche, D. Poppelmonde, R. Merckx, S. Temmerman, and G. Gover. 2018. "Long Term Organic Carbon Sequestration in Tidal Marsh Sediments in Dominated by Old-Aged Allochthonous Inputs in a Macrotidal Estuary." *Global Change Biology* 24: 2498–2512. https://doi.org/10.1111/gcb.14089.

Walden, L., O. Serrano, Z. Shen, et al. 2024. "Mid-Infrared Spectroscopy Determines the Provenance of Coastal Marine Soils and Their Organic and Inorganic Carbon Content." *Science of the Total Environment* 949: 174871. https://doi.org/10.1016/j.scitotenv.2024.174871.

Wigand, C., E. Davey, R. Johnson, et al. 2015. "Nutrient Effects on Belowground Organic Matter in a Minerogenic Salt Marsh, North Inlet, SC." *Estuaries and Coasts* 38: 1838–1853. https://doi.org/10.1007/s12237-014-9937-8.

Xiao, K., Y. Wu, F. Pan, et al. 2024. "Widespread Crab Burrows Enhance Greenhouse Gas Emissions From Coastal Blue Carbon Ecosystems." *Communications Earth & Environment* 5: 437. https://doi.org/10.1038/s43247-024-01621-2.

Yang, R.-M. 2020. "Characterization of the Salt Marsh Soils and Visible-near Infrared Spectroscopy Along a Chronosequence of *Spartina alterniflora* Invasion in a Coastal Wetland of Eastern China." *Geoderma* 362: 114138. https://doi.org/10.1016/j.geoderma.2019.114138.

Supporting Information

Additional Supporting Information may be found in the online version of this article.

Submitted 30 July 2025
Revised 26 November 2025
Accepted 28 November 2025